Progress in Photovoltaics: Research and Applications

WILEY

PROGRESS IN PHOTOVOLTAICS

RESEARCH ARTICLE OPEN ACCESS

Long-Term Photovoltaic System Performance in Cold, Snowy Climates

Erin M. Tonita[1] | Dirk C. Jordan[2] | Silvana Ovaitt[2] | Henry Toal[3] | Karin Hinzer[1] | Christopher Pike[3] | Chris Deline[2]

[1]SUNLAB, University of Ottawa, Ottawa, Ontario, Canada | [2]National Renewable Energy Laboratory, Golden, Colorado, USA | [3]Alaska Center for Energy and Power, University of Alaska Fairbanks, Fairbanks, Alaska, USA

Correspondence: Erin M. Tonita (etoni044@uottawa.ca)

Received: 24 August 2024 | **Revised:** 26 February 2025 | **Accepted:** 7 July 2025

Funding: This work was supported by the Office of Naval Research (N00014-19-1-2235), the Natural Sciences and Engineering Research Council of Canada (NSERC CREATE 497981, NSERC STPGP 521894, and NSERC CGS-D), the Solar Energy Technologies Office (385258 and 38259), and the Office of Energy Efficiency and Renewable Energy.

Keywords: continental | degradation | high latitude | performance loss | performance ratio | photovoltaics | polar | specific yield

ABSTRACT

As countries around the world transition towards renewable energy, there is increasing interest in using photovoltaic (PV) technologies to help decarbonize northern and alpine communities due to their scalability and affordability. However, a barrier to large-scale adoption of PV in cold climates is long-term performance uncertainty under snowfall, freeze–thaw cycles, low temperatures, and high winds. In this work, we provide a comprehensive review of published silicon degradation rates in cold Köppen–Geiger climate classifications of Dfb (humid continental), Dfc (subarctic), and ET (tundra). We first analyze the system degradation rates of three subarctic ground-mounted photovoltaic sites in North America using the RdTools year-on-year method: an Al-BSF double-axis tracking site in Fairbanks, Alaska (65° N); a PERC and silicon heterojunction bifacial vertical and south-tilted site in Fairbanks, Alaska; and a PERC south-facing fixed-tilt site in Fort Simpson, Northwest Territories (62° N). Degradation rates of these newly analyzed sites vary between −0.4%/year and −1.5%/year. Combining these data with previously reported cold climate degradation rates, we show that the distribution of cold climate degradation peaks at −0.1%/year to −0.2%/year but has a large tail with rates above −0.5%/year. The average reported cold climate degradation rate is −0.45%/year, whereas the median value is −0.33%/year. These results suggest that despite frequent freeze–thaw cycles and potential exposure to high wind and snow loads, PV systems in cold climates tend to degrade slower than PV systems in warmer climates. The limited sample size of reported degradation rates in cold climates (27) motivates the need for further data acquisition and monitoring efforts as new technologies are deployed.

1 | Introduction

Photovoltaic (PV) systems have been deployed in high latitude and mountainous regions as early as the 1980s to provide clean, distributed, and scalable energy for buildings and equipment [1, 2]. However, it is only in recent years that the cold climate PV market has begun to see regular PV deployments > 100 kWp in these climatic regions with total regional installed PV capacities in the few to hundreds of MWp range [3–8]. PV systems are being deployed in diverse configurations in high latitudes and altitudes, including in rooftop residential applications [9], building-integrated applications [10, 11], hybrid microgrids

Inclusion and diversity: One or more of the authors of this paper self-identifies as an underrepresented ethnic minority in science.

[12, 13], and centralized grids [14]. Integration of PV into cold climate infrastructure can reduce electricity bills [12, 15], offset diesel consumption and associated greenhouse gas emissions [15–18], peak shave [17], offer dual-land purpose [11, 19], and prepare existing grids for growing electricity demand [20].

PV systems deployed in high latitude and alpine climates will be exposed to low ambient temperatures, moderate to high seasonal snowfall, frequent freeze–thaw cycles, and, in the case of high-latitude cold climates, strong seasonal variations in solar resource, including months of near or total darkness. These meteorological effects may impact the long-term performance of PV systems in cold climates.

For example, snow and ice accumulation on PV arrays exerts a load that is typically nonuniform and irregular in frequency and can last for up to months at a time [21, 22]. Snow load can lead to cell cracking, whereas moisture ingress from melt can lead to delamination and corrosion [21]. Additionally, snow removal practices can cause damage to module surfaces, leading to potential module breakage [23].

Temperature also plays a role in PV system durability. Schneller et al. [24] have shown that a single exposure to −40°C can permanently reduce the fracture strength of crystalline silicon (c-Si) cells. PV materials such as encapsulants and backsheets may experience a glass transition in cold climates [25], with measured glass transition temperatures of ethylene-vinyl acetate (EVA) occurring at −15°C and −35°C in the literature [25, 26]. Cell connectors have also been found to be susceptible to failure during cold temperature thermal cycling down to −40°C [27].

Despite mechanical weakening under exposure to cold temperatures, cold operating temperatures will increase PV system efficiency [28] and can result in other reliability benefits. Maximum power temperature coefficients of c-Si modules today typically lie in the range of −0.25%/°C to −0.40%/°C, causing photovoltaic energy conversion efficiency to increase for colder temperatures [28]. Moreover, cold environments will suppress major thermally activated degradation processes, such as mechanisms related to chemical reactions and diffusion [29]. UV-induced degradation mechanisms, such as encapsulant discoloration, will be less common at high latitudes [30] but could still occur in alpine climates [31].

Here, we review published silicon PV degradation rates for cold Köppen–Geiger climate classifications of Dfb (humid continental), Dfc (subarctic), and ET (tundra) and additionally provide new degradation analysis for three subarctic sites in North America. Several studies have been published in the past that analyze PV module degradation in hot and humid, hot and dry, and warm and temperate climates [31], with degradation rates ranging around −0.75 to −1.2%/year [32–35]. However, existing literature on PV degradation in cold climates is relatively limited, especially for subarctic and tundra climates.

Earlier studies on the impact of climate on PV degradation suggest improved performance in cooler climates. In 2016, Jordan et al. [33] reported a median degradation rate of −0.35%/year (−0.62%/year average) for 26 PV systems in Dfa (hot-summer humid continental), Dfb, Dfc, and ET climates with x-Si technology (a-Si, c-Si, etc.). Half of the analyzed systems were located in Dfa climates.

In 2022, Jordan et al. [32] analyzed performance loss rates (PLRs) for sites deployed in the continental United States and separated results by temperature zone, finding slower PLR for the coolest US temperature zone that had significant PV system data. The coolest temperature zone PV arrays degraded with a median rate of −0.48%/year, compared to two other hotter climate zones (−0.78%/year and −0.88%/year). The coolest temperature zone roughly corresponded to the northern third of the continental United States, excluding continental Alaska, mountainous regions, and many regions close to the northern border with Canada [36]. No subarctic or tundra climates were included in the analysis.

Ascencio-Vasquez et al. simulated PV degradation rates worldwide according to Köppen–Geiger climate classification zones [37] considering three degradation mechanisms: hydrolysis degradation, photo-degradation, and thermo-mechanical degradation [38]. All three degradation mechanisms were found to be reduced in cold climates, resulting in the lowest predicted degradation rates occurring in cold and polar climates with average predicted degradation rates of −0.2%/year. However, the authors warned that these calculations do not include external effects like snow and wind, which may cause increased degradation rates and PLRs in practice [38].

In this work, we first analyze the degradation rates of four diverse PV systems located in three subarctic (>60° N) sites in Alaska and Northern Canada. We analyze the degradation rates of the PV systems using a robust year-on-year degradation methodology, which attempts to account for the strong seasonal variation present at high latitudes [20, 39]. We then include these degradation rates in a compendium of published PV degradation rates for cold climates of Dfb, Dfc, or ET Köppen–Geiger climate classification. We limit our study to only multicrystalline silicon (mc-Si) and c-Si technologies with ≥3 years of outdoor field exposure.

2 | Photovoltaic Sites

Figure 1 shows a map of the three subarctic PV sites studied in this work alongside locations of degradation rate studies in Dfb, Dfc, and ET climates detailed in the compendium (Section 5). The subarctic PV systems analyzed in Fairbanks, Alaska, represent the three highest latitude PV sites analyzed for degradation to date and the first instances of PV degradation analysis in Alaska. In addition, we present the first long-term performance analysis of a subarctic double-axis tracking PV system. Environmental conditions at the three sites are summarized in Table S1.

2.1 | Fort Simpson, Canada

The subarctic PV array analyzed in Canada is located in Fort Simpson, Northwest Territories (61.9° N, 121° W). It consists of 100 kW of ground-mounted fixed-tilt panels at a tilt of 35° and an azimuth of 190°. The array, maintained by the

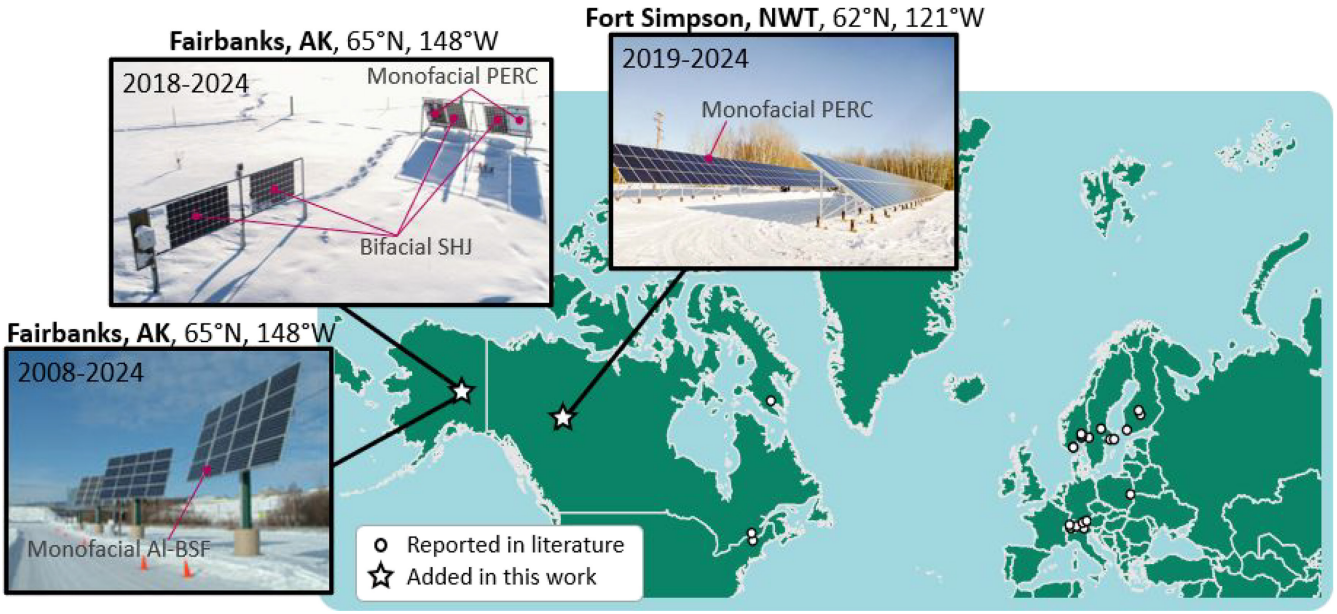

FIGURE 1 | Locations of PV sites discussed in this work. Newly analyzed subarctic PV systems are pictured and denoted by stars. Silicon PV systems located in cold climates (Köppen Geiger climate codes of Dfb, Dfc, and ET), which have published degradation rates for ≥ 3 years of field exposure are given by the circles on the map. Previous studies primarily analyze PV in the Nordic countries and in the European Alps.

Northwest Territories Power Corporation [40], was installed in two phases starting in 2012 and completed in February of 2013 and consists of 258 Conergy ON 235P-235 modules and 178 Conergy ON 245P-245 modules. AC power data are retrieved at the inverter level for the whole array (inverter model Enphase M215 208 V).

Meteorological data collection of module temperature, plane-of-array (PoA) irradiance, and global horizontal irradiance (GHI) began in 2017. Wind speed and ambient temperature are collected at a nearby airport weather station (Fort Simpson A, Climate ID 2202103). Measured power, energy, and meteorological data are at a resolution of 15 min and cover 6 years, from 2017–2023. Thermopile, PoA, and GHI pyranometers are calibrated yearly at the site. Snow is removed periodically in March from the array.

2.2 | Fairbanks, United States—Fixed Tilt

The second analyzed subarctic PV site is a ground-mounted south-facing and east–west vertical fixed-tilt site in Fairbanks, Alaska (64.8° N, 147.7° W), consisting of six modules, each connected to an Enphase IQ6 microinverter. PV production is measured on the AC side. Four of the modules are silicon heterojunction (SHJ) modules, Sunpreme Maxima GxB-310 with 94% bifaciality. The remaining two modules are monofacial passivated emitter rear-contact (PERC) modules, Suniva OPT270-60-4-1B0. All modules were flash tested before outdoor exposure, with the average maximum power under standard test conditions of the bifacial and monofacial modules being 288 and 251 W, respectively. The Alaska Center for Energy and Power of the University of Alaska, Fairbanks, maintains the array. Further details on the site, including a performance comparison of east–west vertical to south-tilted modules, can be found in Ref. [41].

Meteorological and PV production data have been collected at 1-min resolution for 5 years from 2019–2024. Ambient temperature, wind speed, albedo, GHI, and PoA irradiance are measured on site. An example year of meteorological data for this site is provided in Figure 2, demonstrating strong seasonal effects for GHI (Figure 2A), ambient temperature (Figure 2B), and albedo (Figure 2D). The site and meteorological station are serviced on a roughly weekly schedule.

2.3 | Fairbanks, United States—Double-Axis Tracking

The final subarctic PV site analyzed in this work is a double-axis tracking ground-mounted site in Fairbanks, Alaska. This site consists of four double-axis trackers commissioned in 2007 by the Cold Climate Housing Research Center (CCHRC), now known as the National Renewable Energy Laboratory (NREL) Alaska Campus. The arrays have been continuously monitored at an hourly resolution since their commissioning, resulting in 16 years of data from 2008–2024. Data for this site are publicly available and can be found at Ref. [42]. For this analysis, we analyze three of the four arrays, neglecting one array that has an experimental design combining mc-Si cells with concentrating optics.

Each of the three studied trackers consists of 16 modules and is referred to as Arrays 1–3 in this work. Arrays 1 and 2 consist of SolarWorld 165 mc-Si modules with a rated power of 2640 W each. Array 3 uses Sharp 170 mc-Si modules with a rated power of 2720 W. These arrays were originally constructed to demonstrate the difference in energy payback periods for double-axis trackers compared to south-facing fixed-tilt trackers. A direct comparison between Arrays 1 and 2 was done for this purpose [43], with Array 1 performing double-axis tracking and Array 2 purposefully fixed to a south-facing tilt for the first 2 years of

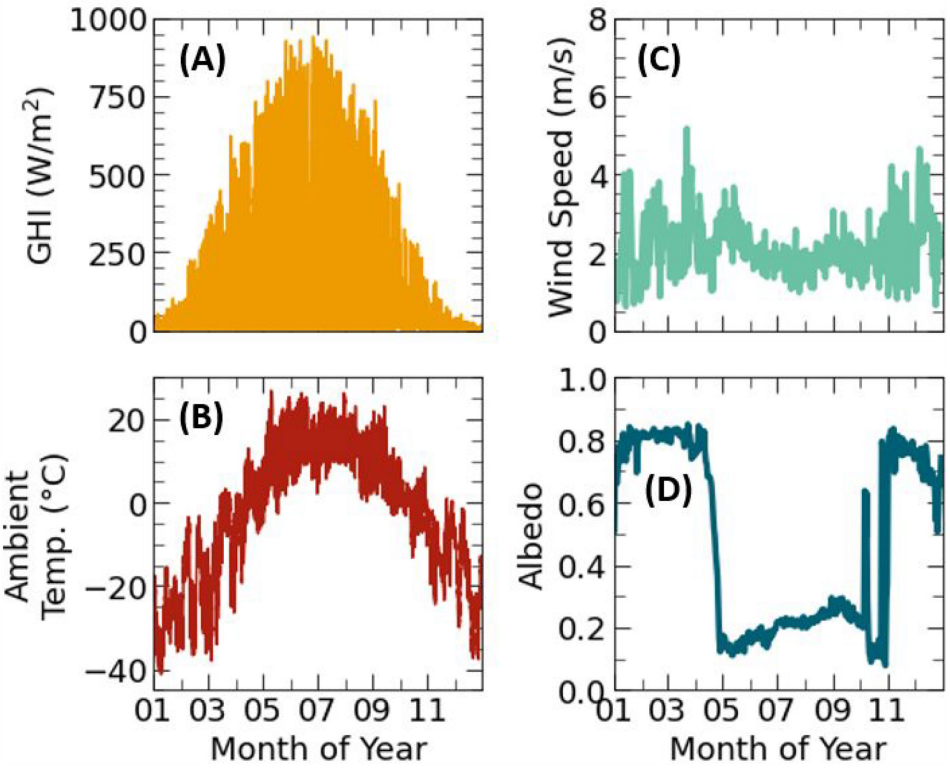

FIGURE 2 | An example year of meteorological station data for the fixed-tilt Alaskan array of six modules. (A) Measured GHI, (B) ambient temperature, (C) wind speed, and (D) albedo. Data have been shifted to accommodate a full year without data gaps; August–December months come from 2019 and January–July from 2020. To better show the wind speed and albedo values, daily averages are plotted.

operation. After this experiment, all arrays were set to perform double-axis tracking, except for winter months, where the arrays are south-facing at a fixed-tilt (roughly October through March each year).

PV production data are collected from three SMA Sunny Boy inverters. Module temperature and PoA irradiance are collected on site, whereas wind speed and ambient temperature are measured at a nearby rooftop meteorological station. Due to long-term data quality issues with the available AC power data, the following degradation analysis is completed using measured AC current. This should introduce only modest uncertainty, to the extent that grid voltage remains stable over the measurement period.

3 | Year-On-Year Methodology

To analyze the degradation rates of the three subarctic PV sites, the open-source python-based package RdTools is used [44]. This tool uses a year-on-year methodology to calculate PV array degradation and statistics. This method calculates a system degradation rate that excludes certain performance factors but includes others. To achieve a relatively stable performance estimate, system production is corrected for solar resource and module temperature. Exogenous factors such as grid and maintenance outages are removed. Module degradation driven by changes in chemical composition, cell cracking, and permanent soiling are retained. System degradation losses such as other DC health degradation (string or module failures) and tracker errors are also typically retained. RdTools attempt to remove snow loss effects through normalized filtering, though some snow effects may be retained. As RdTools output includes some performance loss factors and excludes others such as outages, clipping, and seasonal shade or soiling losses, it has been suggested that it does not match other definitions of system PLR [45]. We therefore provide some specifics of the analysis process here.

The RdTools year-on-year methodology relies on four main steps: data normalization, data filtering, data aggregation, and finally, calculation of year-on-year degradation. Figure 3 shows a schematic representation of each of these steps using data for a bifacial SHJ south-facing tilted module in Fairbanks, Alaska.

First, data are normalized against a PV energy yield model, PVWatts [46], to account for changes in temperature and solar insolation from year to year using inputs of measured PoA irradiance, module temperature, the module temperature coefficient, the nameplate DC power, the array longitude and latitude, location time zone, and PV array orientation and tilt. Year-to-year variation from changes in solar spectral content and albedo is not captured by this model. An example of the measured versus PVWatts modeled module power is displayed in Figure 3A for a few days in September of 2019.

Data are then filtered to only include clear-sky timestamps using a built-in function *detect_clearsky* in pvlib [47, 48]. Effectively, measured PoA is compared to a clear-sky model with moving windows where a point is judged clear-sky if agreement is reached within specific tolerances [49]. Next, clipping events

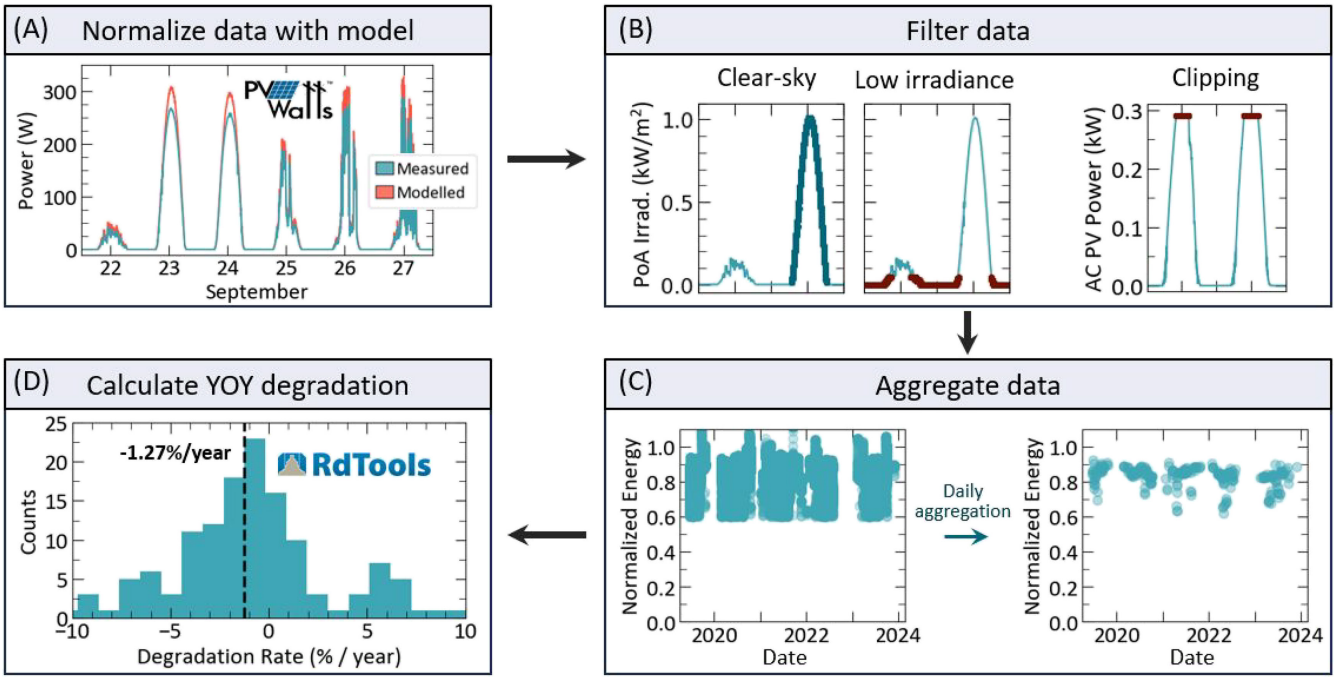

FIGURE 3 | Schematic outlining the main four steps in the year-on-year degradation methodology: (A) normalization, (B) data filtering, (C) data aggregation, and (D) the calculation of degradation rate distribution. YOY, year on year.

are filtered from the data by removing data points where output power is within 99% of the maximum measured power. Low irradiance timestamps $< 50\,W/m^2$ are then removed. A range of low irradiance cutoffs has been recommended in the literature [20, 39, 50]. Karttunen et al. [20] observed that an irradiance cutoff of $200\,W/m^2$ would exclude > 50% of their measured datapoints in Turku, Finland, limiting seasonal analysis and potentially decreasing PLR accuracy. Thus, for this work where PV arrays are located above 60° N, we select an irradiance cut-off of $50\,W/m^2$. Finally, data where PV system energy yield are < 60% of the model-predicted energy yield is removed from the analysis. This filters out significant snow accumulation events, shading from nearby objects, and PV system outages. Impacts from minor snow accumulation will be retained, contributing to some seasonal variation in the normalized data (Figure 3C).

Data are then aggregated to daily irradiance and temperature-weighted averages to reduce high error data from morning and evening timestamps. This step is visualized in Figure 3C. Data aggregation has been shown to reduce degradation rate calculation uncertainty [39].

Finally, the year-on-year degradation rate is calculated by comparing daily aggregated values from year to year, resulting in the distribution of degradation rates as shown in Figure 3D. We report the average of this distribution as the long-term degradation of the system.

PV degradation rate analysis methodologies for high latitude and alpine locations will have higher uncertainty than when they are used for lower latitude and warmer climates. Diffuse fraction tends to increase with latitude in the United States and Canada [51]. Thus, clear-sky filtering in RdTools in high latitude regions results in fewer daily aggregated points and higher degradation rate uncertainties. Calculating the system's year-on-year degradation rate after more years of field exposure will compensate for this data loss. In addition, snow accumulation effects are difficult to entirely remove from analyses without continuous snow monitoring. Data filtering conditions must be selected to balance data retention with data quality.

Despite increased uncertainty, the RdTools year-on-year method is robust to most seasonal change and data outliers and has the benefit that it does not rely on the need to flash test modules in potentially remote areas where access to specialized testing equipment may be limited. Thus, this algorithm is an appropriate choice for assessing PV system degradation rates in cold climates when sufficient field data are present.

4 | Subarctic Pv Site Analysis

Here, we report on PV site data availability, tracking availability, specific yield, and year-on-year degradation for each new subarctic PV site introduced in Section 2 and visualized in Figure 1. We have additionally calculated average monthly performance ratios for these PV systems, which is presented in Figure S1.

4.1 | Site Availability and Tracking Availability

Table 1 outlines the availability of site power data and site meteorological station data for the duration of the data acquisition periods. Availability is calculated as the number of timestamps with data divided by the number of timestamps within the data acquisition period. Meteorological station availability is determined by the lowest value between essential temperature and irradiance variable availability.

TABLE 1 | Summary of site power and meteorological data availability.

Site	Years in operation	Data resolution	Site data availability (%)	Met. station availability (%)
Fort Simpson, Canada South fixed-tilt array	6	15 min	2001/2191 days = 91	2001/2191 days = 91
Fairbanks, USA Fixed-tilt modules	5	1 min	1572/1656 days = 95	1391/1656 days = 84
Fairbanks, USA Double-axis tracker heads	16	1 h	5326/5582 days = 95	3653/5582 days = 65

TABLE 2 | Summary of annual Alaskan double-axis tracking site tracker availability. Tracking is disabled in the winter, leading to a maximum annual availability of 61%.

	Double-axis tracking availability (%)	
	Annual	Nonwinter months
Array 1	51	86
Array 2	43	63
Array 3	37	48

Because power and weather data from Fort Simpson for the south-tilted array were provided together, the availability of data is the same for both site data and meteorological data at 91%. For the east–west vertical and south-facing fixed-tilt site in Fairbanks, site data availability is 95%, whereas meteorological station availability is 84%. Since 2008, the double-axis tracking site in Fairbanks has had a data availability of 95% and a meteorological station availability of 65%. Data gaps primarily occur from 2014 to 2018 for the PoA sensors. There was an additional loss in data around 2015–2017 in wind speed and ambient temperature. This data loss may be due to issues with long-term maintenance of the site database.

We additionally report on the availability of the tracking system for the double-axis tracking site in Fairbanks over the past 16 years in Table 2. The azimuth and elevation of each tracker were monitored throughout the study with the same data availability as the meteorological station. When the arrays are not tracking, each tracker is fixed to an azimuth of between ~150° and 180° and a tilt of ~60°–74°. Array tracking is disabled each year from roughly October through March to reduce reliability concerns with moving parts during the winter months. Given this constraint, the best annual tracking availability possible is 61% of the year. When tracking is enabled, the double-axis tracking arrays successfully tracked the sun between 48% and 86% of the time, depending on the array. Array 3 experienced a tracking failure in 2019 and has not been tracking since, resulting in an annual tracking availability of 48%.

4.2 | Specific Yield

Figure 4 shows the calculated annual specific yield from each site in each configuration. Specific yield is calculated as the yearly average energy produced by the PV array divided by the rated power. For the east–west vertical and south-tilted site in Fairbanks (Figure 4A), bifacial east–west vertical panels and bifacial south-tilted panels have comparable performance with a specific yield of ~1200 kWh/kWp. Bifacial gain falls between 27% and 34% annually compared to the monofacial modules.

The annual specific yield for the double-axis tracking site in Fairbanks is given in Figure 4B for fixed-tilt and double-axis tracking configurations. These values are calculated using the annual energy yield for the first 2 years between Arrays 1 and 2, as reported in Ref. [43]. Double-axis tracking leads to a 41% increase in annual energy yield, which is interestingly the same value reported by Burnham et al. for a double-axis tracking site located at 44° N in Vermont [52].

The specific yield of the monofacial south-tilted site in Fort Simpson is 1067 kWh/kWp, visualized in Figure 4C.

4.3 | Year-On-Year Degradation Rates

Finally, degradation rates are calculated for each subarctic site using the methodology outlined in Section 3. A degradation rate is calculated per module in the east–west vertical and south-tilted Fairbanks PV site (Figure 5A), per tracker in the double-axis tracking Fairbanks PV site (Figure 5B), and for the overall fixed-tilt PV array in Fort Simpson (Figure 5C). A dashed line is provided at a rate of zero in Figure 5. Each data point is provided with error bars given by a 68.2% confidence interval.

For the fixed-tilt site in Fairbanks (Figure 5A), we average degradation rates for the bifacial SHJ modules and the monofacial PERC modules separately. With this small sample size (4), there is no clear difference between modules of the same type oriented either vertically (P1 and P2) or south-tilted (P3 and P4). Bifacial SHJ modules may be degrading faster than the monofacial PERC modules in Fairbanks at −1.25%/year (SHJ) compared to −0.58%/year (PERC). Monofacial PERC degradation rates are reported to typically fall between −0.5%/year and −0.9%/year [53, 54], whereas SHJ median degradation rates are −0.8%/year [55]. Though the Fairbanks SHJ modules (Sunpreme GxB 310) are degrading faster than this median value at −1.25%/year, the degradation rates of similar modules (Sunpreme HxB 400) in a warmer climate have been

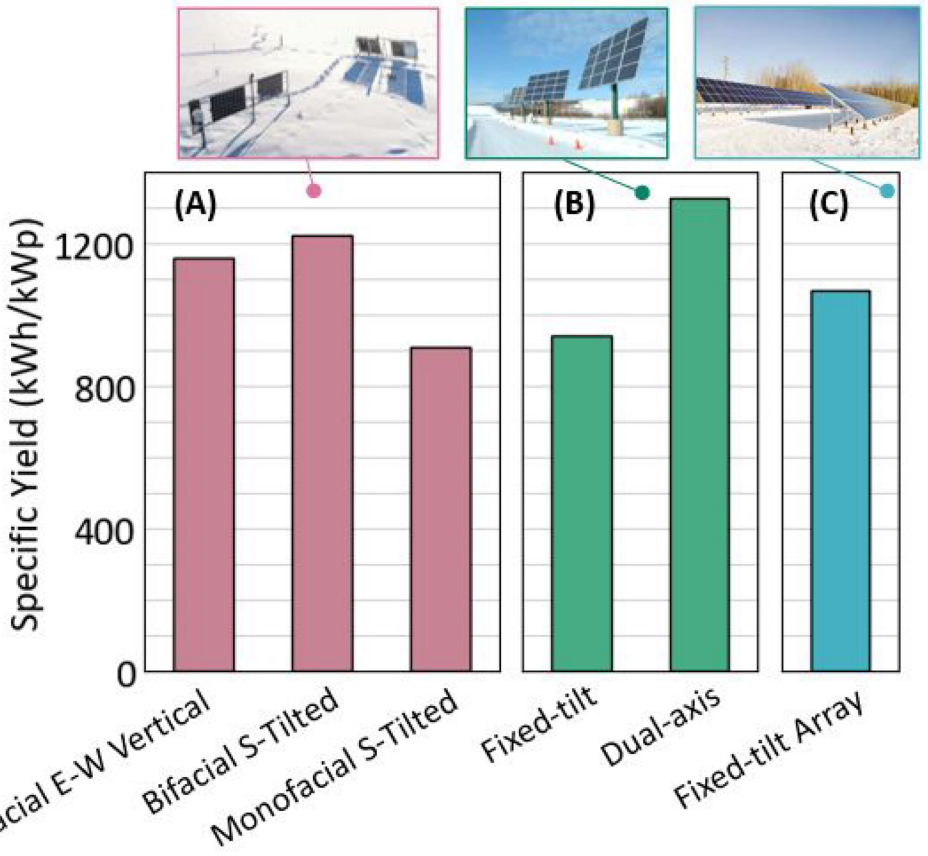

FIGURE 4 | Specific yield for the various configurations at each subarctic site. (A) Average specific yield for pairs of modules in bifacial east–west vertical, bifacial south-tilted, and monofacial south-tilted configurations in Fairbanks, Alaska. (B) Specific yield of Alaskan double-axis trackers Arrays 1 and 2 from 2007 to 2009 when in south-facing fixed-tilt and dual-axis tracking modes. (C) Specific yield of the monofacial south-tilted site in Fort Simpson, Canada.

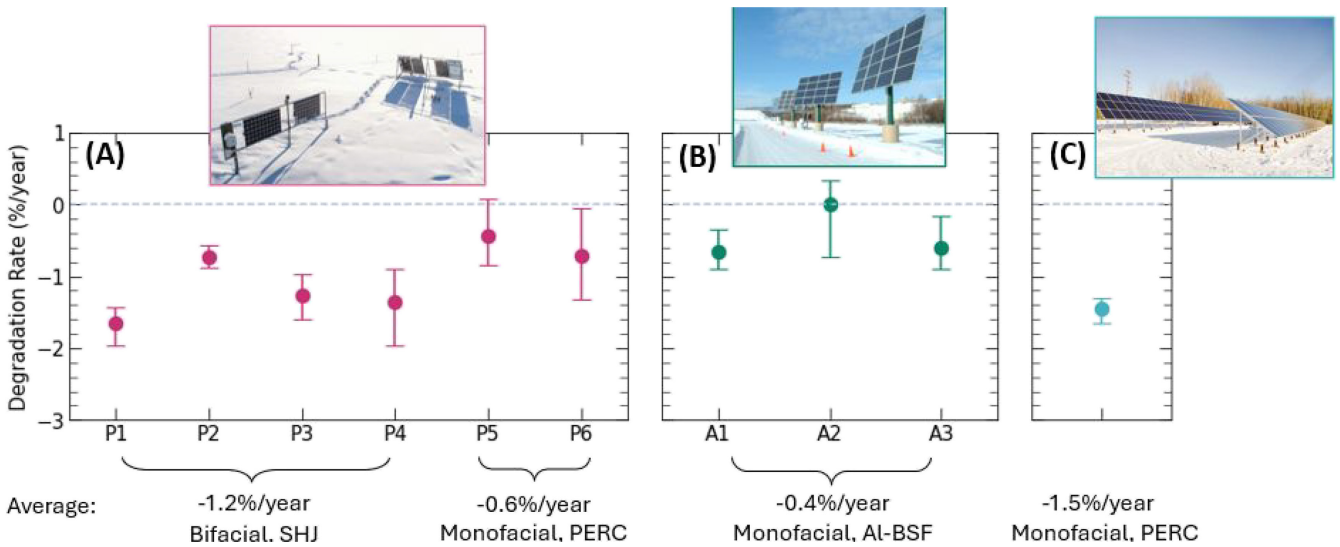

FIGURE 5 | Year-on-year degradation rates for (A) east–west vertical (P1 and P2) and south-tilted (P3–P6) modules in Fairbanks, Alaska; (B) double-axis tracking arrays in Fairbanks, Alaska; and (C) the fixed-tilt array in Fort Simpson, Northwest Territories. Error bars are given by a confidence interval of 68.2% for each data point.

degrading quicker at a rate of −1.9%/year [56]. Further studies on emerging bifacial SHJ modules are recommended in diverse climate zones to determine the impact of climate on observed degradation.

For the double-axis tracking arrays in Fairbanks, an average AC current degradation rate of −0.4%/year is observed (Figure 5B). There have been some noted observations of glass damage to the modules caused by the impact of gravel from the nearby gravel

road. In remote locations where gravel roads are common, it is recommended to provide greater distance between PV arrays and roads.

Finally, in Fort Simpson (Figure 5C), the year-on-year array degradation is −1.5%/year. Because data are collected and analyzed on the AC side of the inverter, this degradation rate may include degradation from inverter electronics.

The degradation rates reported in this analysis demonstrate the diversity of PV system configurations present in cold climate locations, including significant differences in system age and technology. This is reflected in their largely varying degradation rates, between −0.4%/year and −1.5%/year.

5 | Compendium of Cold Climate Degradation Rates

Here, we review existing literature on the degradation of mc-Si and c-Si PV systems located in Köppen–Geiger Dfb, Dfc, and ET climate codes with ≥3 years of field exposure [37]. A literature survey has been conducted for this purpose to the best of the authors' ability, finding 19 publications covering 23 PV systems in cold climates [1, 2, 10, 20, 57–71]. Any arrays with substring degradation rates are reported here as a median value for the PV system to highlight differences between systems and reduce data bias towards PV arrays with multiple strings of data. Including the four unique PV systems studied in this work, the total number of analyzed PV systems is 27.

The reported values in this compendium include both degradation rates, for example, for studies conducted using measured I-V parameters before and after field exposure, PLRs, and analysis methodologies that fall in-between these two, such as RdTools described in Section 3. Studies primarily aim to analyze degradation rate methodologies via module I-V flash-testing or sophisticated year-on-year approaches; however, a mix of other approaches for filtering data and removing seasonal effects are present in the literature. This is further discussed in Section 5.1.2 below. For simplicity, in this article, we refer to all these results together as degradation rates.

Details on each PV system included in this compendium are summarized in Table 3 in order of latitude. Table 3 includes information on array location, Köppen–Geiger climate code, years of analysis, degradation analysis method, installed system capacity, system orientation and mounting, and observed issues mentioned in the publication relating to system performance. In Table 3, the column labeled "data" describes which variable the degradation analysis was conducted on, for example, AC or DC power.

5.1 | Characteristics of Cold Climate Studies

5.1.1 | Site Locations and Climates

Studied PV systems span latitudes from 44° N to 65° N (this work) and include systems in the United States [57], Canada [58, 71], Poland [62], Norway [63, 64, 67, 68], Sweden [2, 65, 66, 69], Finland [20, 70], and the Alps mountain range in Switzerland [1, 10, 59], Germany [60, 61], and Italy [57]. Figure 6A summarizes the distribution of Köppen–Geiger climate codes for the PV system locations, and Figure 6B shows a boxplot of degradation rates per climate code. Due to a small number of systems per climate code category, it is difficult to ascertain if there are distinct degradation trends between climate codes, with degradation rates of −0.32%/year (Dfb), −0.50%/year (Dfc), and −0.19%/year (ET). Similarly, no clear differences are observed in the dataset for cold climates located at high altitude (average −0.42%/year) compared to cold climates located at high latitude (average −0.46%/year).

A separate climate classification for PV systems has been proposed by Karin et al. [36] to replace Köppen–Geiger climate codes called the Photovoltaic Climate Zones (PVCZ). The PVCZ open-rack temperature zones are provided for comparison in Figure 6C/D using the PVCZ python package. Temperature zones were calculated by Karin et al. by modeling the Arrhenius-weighted module temperature for a module in a horizontal open-rack configuration with a polymer backsheet using grided land data for ambient temperature, irradiance, and wind speed. Temperature zones for the locations in this work are limited by the resolution of the grid (0.25°), particularly in alpine locations where a small spatial distance can result in a significantly different climate due to altitude. Temperature zones correspond to average modeled module temperatures of < 14 °C (T1), 14–19 °C (T2), 19–24 °C (T3), and 24–29 °C (T4). Half of the locations identified as T4 are in alpine regions, which the limited spatial resolution of the dataset may have misidentified.

5.1.2 | Analysis Methodology

Figure 6E/F summarizes the analysis methodology used for calculating the degradation rate of each cold climate PV system. In seven studies, a degradation rate was not specifically reported; however, it was possible to digitize the published data to calculate the performance loss. In these cases, the analysis method is described as "calculated from paper," abbreviated as "Calc." in Figure 6C. Often, these calculations were done by analyzing several years of published monthly performance ratio data; thus, these values represent a PLR rather than an irreversible degradation rate, as this analysis does not filter out effects such as soiling, snow accumulation, or shading. The true degradation rate of these reported systems likely is lower than what has been calculated, due to inclusion of these performance-decreasing effects.

The most common method for degradation analysis in the literature for cold climates is using a year-on-year approach, closely followed by comparing I-V measurements before and after field exposure. These two methodologies aim to report the underlying degradation rate of the PV system, with year-on-year methodologies requiring a sophisticated approach to filter out common reversible PV system effects (see Section 3).

Several other analysis methods were found in the studies, offering a mix of PLR calculations and more sophisticated approaches for data filtering. Mutungi [70] used an autoregressive integrated

TABLE 3 | Existing cold climate degradation studies in the literature.

Ref.	Location	Köppen–Geiger Code	PLR (%/year)	Years covered	Analysis method	Data	Module information	System configuration	Reported issues
This work	Fairbanks, USA (64.8° N, 148° W)	Dfc	−1.2 ± 0.4	5 years, 2019–2024	Year-on-year, RdTools	AC power, minutely	1.15 kWp c-Si, bifacial SHJ	Ground, 60° tilt, 180° azimuth, and 90° tilt, 90/270° azimuth	
	Fairbanks, USA (64.8° N, 148° W)	Dfc	−0.6 ± 0.2	5 years, 2019–2024	Year-on-year, RdTools	AC power, minutely	502 Wp c-Si, monofacial and bifacial PERC	Ground, 60° tilt, 180° azimuth	
	Fairbanks, USA (64.8° N, 148° W)	Dfc	−0.4 ± 0.4	16 years, 2008–2024	Year-on-year, RdTools	AC current, hourly	10 kWp mc-Si, Al-BSF	Ground, 4 dual-axis trackers	Some visual damage of modules due to gravel impact from nearby road; JX Crystals array failed after 4 years.
[71]	Iqaluit, Canada (63.8° N, 69° W)	ET	−0.17	9 years, 1995–2004	Calculated from paper	AC energy, annual	3.2 kWp c-Si	Façade, 230° azimuth	
[70]	Saarijärvi, Finland (62.7° N, 25° E)	Dfc	−0.33	7 years, 2005–2013	ARIMA	AC power, minutely	6.27 kWp c-Si, SHJ	Rooftop	Small interruptions from inverter errors.
	Jyväskylä, Finland (62.2° N, 26° E)	Dfc	−0.1	3 years, 2009–2013	ARIMA	AC power, minutely	2.6 kWp mc-Si	Rooftop, 40° tilt, 180° azimuth	Small interruptions from inverter errors.
This work	Fort Simpson, Canada (61.9° N, 121° W)	Dfc	−1.5	6 years, 2018–2024	Year-on-year, RdTools	AC power, 15-min	100 kWp c-Si, monofacial PERC	Ground, 35° tilt, 190° azimuth	Missing first 5 years of operation data.
[69]	Borlänge, Sweden (60.6° N, 16° E)	Dfb	−0.5	30 years, 1994–2024	IV before & after	IV parameters	3.2 kWp mc-Si	Rooftop, 60° tilt, 210° azimuth	Light module yellowing, with otherwise no visual damage reported.
[20]	Turku, Finland (60.5° N, 22° E)	Dfb	−1.46	4 years, 2017–2021	Year-on-year	DC power, minutely	375 Wp c-Si, bifacial	Rooftop, 90° tilt, 90° azimuth	Suspected possible PID.
[68]	Oslo, Norway (60.0° N, 11° E)	Dfb	−0.41	6 years, 2017–2023	Year-on-year, RdTools	AC power	720 Wp mc-Si	Rooftop, 10° tilt	
	Oslo, Norway (59.8° N, 11° E)	Dfb	−0.15	8 years, 2015–2023	Year-on-year, RdTools	AC power	370 Wp mc-Si	Rooftop, 10° tilt	
[67]	Vestby, Norway (59.6° N, 11° E)	Dfb	−0.14	5 years, 2015–2019	Year-on-year	DC power, 5 min	120 kWp mc-Si	Rooftop, 10° tilt, 112° azimuth	

(Continues)

TABLE 3 | (Continued)

Ref.	Location	Köppen–Geiger Code	PLR (%/year)	Years covered	Analysis method	Data	Module information	System configuration	Reported issues
[66]	Glava, Sweden (59.6° N, 13° E)	Dfb	−0.22	10 years, 2012–2022	Clear sky peak power degradation	Power, 6 days per year	No info	No info	Missing first 3 years of operation data.
[65]	Huvudsta, Sweden (59.3° N, 18° E)	Dfb	0	21 years, 1985–2007	IV before & after	IV parameters	2.1 kWp mc-Si	Façade	No visual defects.
[2]	Stockholm, Sweden (59.3° N, 19° E)	Dfb	−0.17	25 years, 1981–2006	IV before & after	IV parameters	660 Wp mc-Si	Rooftop/façade	Some encapsulant bubbling, corroded contact grids; one case of minor delamination; one module with hotspot failure.
[64]	Grimstad, Norway (58.3° N, 8° E)	Dfb	−0.17	4 years, 2014–2018	IV near STC	IV parameters	940 W mc-Si	Rooftop, 39° tilt	Degradation mostly from short-circuit current.
[63]	Grimstad, Norway (58.3° N, 8° E)	Dfb	−1.0	10 years	IV before & after	IV parameters	1.0 kWp mc-Si	Rooftop, 58° tilt, 180° azimuth	
[62]	Poland (51.9° N, 23.2° E)	Dfb	−0.07	4 years, 2015–2018	Calculated from paper	Specific yield, annual	21.3 kWp mc-Si	Ground, 34° tilt, 180° azimuth	
[61]	Wendelstein, Germany (47.7° N, 12° E)	ET	0	3 years, 1991–1994	Calculated from paper	PR, monthly	31.5 kWp mc-Si and c-Si	Ground, 60° tilt	
[60]	Zugspitze, Germany (47.4° N, 11° E)	ET	−0.37	3 years	IV before & after	IV parameters	7 modules	Rooftop, 45° tilt	Some cell breakage; one metal frame destroyed by snow and ice; high snowfall and wind.
[59]	Burgdorf, Switzerland (47.1° N, 8° E)	Dfb	−1.09	8 years, 2002–2010	Calculated from paper	DC efficiency, monthly	3.18 kWp c- Si	Rooftop, 30° tilt	
[1]	Domat, Switzerland (46.8° N, 9° E)	Dfb	−0.58	12 years, 1989–2002	Calculated from paper	Energy yield, monthly	104 kWp mc-Si	Sound barrier, 45° tilt, 180° and 155° azimuth	Leakage current found under wet conditions; inverter failure after 11 years; 21 modules damaged and 12 modules stolen during operation.

(Continues)

TABLE 3 | (Continued)

Ref.	Location	Köppen–Geiger Code	PLR (%/year)	Years covered	Analysis method	Data	Module information	System configuration	Reported issues
[10]	Birg, Switzerland (46.6°N, 8° E)	ET	−0.19	8 years, 2002–2010	Calculated from paper	DC efficiency, monthly	c-Si	Rooftop, 90° tilt	
[59]	Jungfraujoch, Switzerland (46.6°N, 8° E)	ET	−0.19	10 years, 1993–2004	Calculated from paper	PR, 5-min	1.15 kWp c-Si	Façade, 192° and 207° azimuths	Windstorms of 250 km/h; irradiance peaks > 1700 W/m^2; some instances of delamination from moisture ingress.
[57]	Bolzano, Italy (46.5°N, 11.3° E)	Dfb	−0.5	8 years, 2011–2019	Average of various methods	AC power	4.2 kWp mc-Si	Ground, 30° tilt, 180° azimuth	Missing first 6 months of operational data
[58]	Varennes, Canada (45.7°N, 73°W)	Dfb	−0.6	23 years, 1992–2015	IV before & after	IV parameters	16.7 kWp c-Si	Rooftop, 45° tilt	Freeze–thaw led to moisture ingress, busbar corrosion.
[57]	Williston, USA (44.4°N, 73.1°W)	Dfb	−0.03	3 years, 2015–2018	Average of various methods	AC power	3.2 kWp mc-Si	Ground, 35° tilt, 180° azimuth	

moving average (ARIMA) method to calculate the degradation rates for two sites in Finland. This methodology removes outages and includes some seasonality. Rinio et al. [66] analyzed six clear sky days per year for a 10-year-old site in Sweden to calculate site performance loss. French et al. [57] reported the degradation rate for two cold climate sites by taking an average of several analysis methods and data filters, including using a year-on-year approach and seasonal and trend decomposition with Loess. The diverse methodologies highlight the variability in degradation analysis approaches, underscoring the need for standardized methods to improve comparability and accuracy across studies.

5.1.3 | PV System Configuration and Capacity

Cold climate degradation studies have primarily been conducted to date on small rooftop deployments. Figure 6G categorizes the number of studies conducted on rooftop, ground-mounted, and façade PV systems, whereas Figure 6H summarizes the degradation rates reported for each configuration. The mounting environment of a PV system will impact the thermal environment of the modules and thus can influence module degradation rates [33, 72, 73]. As rooftop PV systems tend to operate at higher temperatures, degradation rates for roof-mounted PV can be higher [33, 72, 73]. In this dataset of Dfb, Dfc, and ET climate code PV systems, we find that rooftop PV systems have a median degradation rate of −0.35%/year compared to ground-mounted PV systems at −0.50%/year. More data are required to draw stronger conclusions on the effect of mounting configuration in cold climates.

The distribution of PV capacities studied is given in Figure 6I/J. In several cases, no data were provided on the system size. This is denoted as "no info." Around 20% of all studies were conducted for small and experimental systems <1 kWp, and 40% of the studies were conducted on PV arrays with capacities between 1 and 10 kWp. The largest studied PV system in a Dfb, Dfc, or ET climate zone is a 120-kWp rooftop array in Vestby, Norway [67].

5.1.4 | Field Exposure and Deployment Decade

Figure 6K shows the number of years of field exposure of the PV systems studied, and Figure 6L shows the degradation rates for each exposure bin. Because we have excluded any studies with less than 3 years of data, field exposure time is categorized unevenly from 3–5, 5–10, 10–15, and 20+ years. Only five systems have been studied in Dfb, Dfc, or ET climates after ≥15 years of field exposure: a rooftop array in Varennes, Canada [58]; a rooftop and façade array in Stockholm, Sweden [2]; a façade array in Huvudsta, Sweden [65]; a rooftop array in Borlänge, Sweden [69]; and the double-axis tracking site presented in this work in Fairbanks, Alaska. Most studies in the compendium are for PV systems with field exposure between 5 and 10 years in length.

The decade of PV system deployment is provided in Figure 6M/N, with PV systems deployment dates ranging from 1981 to 2019 in this compendium. Figure 6N demonstrates a rise in PV

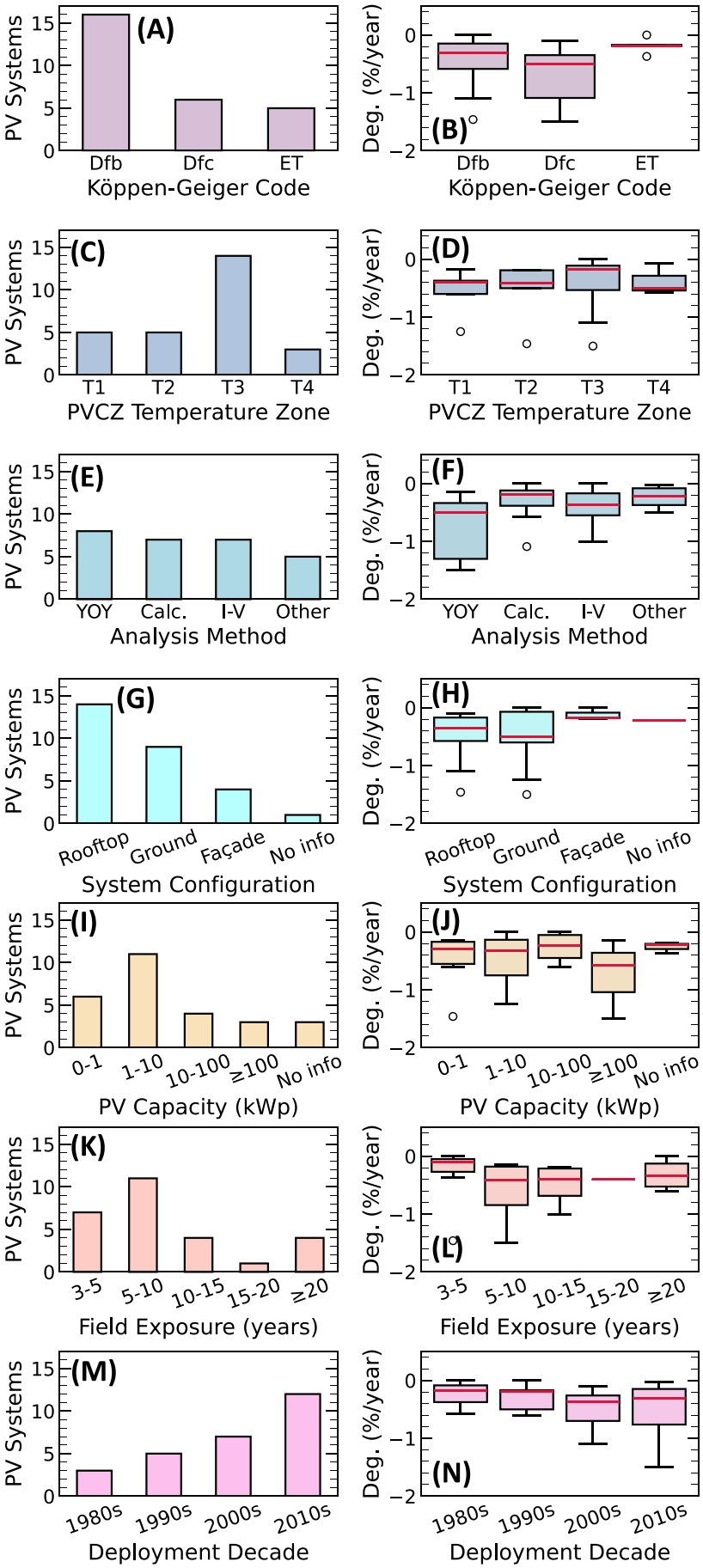

FIGURE 6 | Legend on next page.

FIGURE 6 | The distribution of cold climate PV systems and boxplots by various categories: (A, B) Köppen–Geiger climate classification, (C, D) PVCZ temperature zone classification, (E, F) degradation analysis methods, (G, H) system configurations, (I, J) PV system capacity, (K, L) field exposure, and (M, N) deployment decade. Horizontal red lines in the boxplots denote the median value for each category. In subplots, (E, F) degradation analysis methods are abbreviated, with "Calc." referring to the number of PV systems where degradation rates were calculated by the authors of this work from data provided in publications. "I-V" refers to the measurement of current–voltage parameters before and after field exposure.

degradation rates in time, with median (average) degradation rates increasing from −0.17%/year (−0.25%/year) in the 1980s to −0.32%/year (−0.54%/year) in the 2010s. The number of PV systems studied is also increasing in recent decades (Figure 6M), which is an indication of the rise in interest in PV system deployments in cold climates in time.

The observed increase in PV system degradation in time may be due to historic trends in module architecture towards larger formats, thinner silicon wafers, and thinner glass sheets. Together, these effects can reduce the mechanical durability of modules and result in more cell-cracking, glass-cracking, and module contortion in time [29, 74]. Continued reliability testing and development of appropriate standards for cold climate conditions are required to ensure module durability for emerging designs.

5.1.5 | Degradation Rates

Finally, the location and distribution of all reported degradation rates for mc-Si and c-Si PV arrays in cold climate zones of Dfb, Dfc, and ET with ≥3 years of field exposure are provided in Figure 7. The locations of cold climate degradation studies are shown in Figure 7A, and a histogram of reported rates is provided in Figure 7B.

Most studies report a degradation rate of between −0.1%/year and −0.2%/year; however, there is a long tail in the distribution with faster observed degradation rates. The median degradation rate of cold climate sites is found to be −0.33%/year, whereas the mean is −0.45%/year, reflecting the influence of this long tail.

5.1.6 | Observed Degradation Mechanisms

Issues related to moisture ingress were identified in several of the cold-climate PV sites [1, 2, 10, 58]. Bogdanski et al. [60] reported on a module frame that was destroyed by snow and ice freeze–thaw in Zugspitze, Germany. Cell and glass damage has also been reported in a couple of instances [60], including damage noted by the authors of this work for the double-axis tracking PV site located in Fairbanks, Alaska, near a gravel road.

5.2 | Global Context

The number of PV system degradation studies in cold climates is relatively limited compared to other, warmer climates. Figure 8 summarizes the reported median degradation rates for three other published reviews, which include Dfb, Dfc, or ET Köppen–Geiger climate codes.

Lindig et al. [75] reported the average PLR of Dfb PV systems in Europe from the PV PEARL database (purple circle in Figure 8). The median PLR was found to be −0.17%/year for 19 mc-Si, c-Si, and thin film systems with an average field exposure of 2.8 years. The authors also examined warmer temperate climate zones of Cfa, Cfb, and Csa, reporting PLRs between −0.63%/year and −1.55%/year for these climate zones using a year-on-year analysis [72, 75].

In 2022, Jordan et al. [32] analyzed 1700 utility-scale PV systems in the continental United States [32]. A subset of the sites was analyzed for PLRs by PVCZ temperature zone, finding lower PLRs for the northern third of the United States (44 sites, blue circle in Figure 8). PV arrays located in this region degraded with a median PLR of −0.48%/year, compared to the middle (−0.78%/year) and southern (−0.88%/year) third of the continental United States. The northern third of the United States primarily consists of Dfa, Dfb, and BSk Köppen–Geiger climate zones, as noted in Figure 8, though other climates may also be included in this analysis.

In 2016, Jordan et al. [33] published a summary of reported degradation rates around the globe, finding around 200 studies and 11,000 degradation rates, but with only 39 data points attributed to snowy regions (Dfa, Dfb, Dfc, and ET climates). The 39 snowy data points reported by Jordan et al. [33] consisted of thin-film, mc-Si, and c-Si studies with multiple strings of data with a median degradation rate of −0.35%/year (−0.62%/year average). These 39 data points represent 26 unique PV systems, as plotted in Figure 8. Moderate, hot and humid, and desert climate types were also reported with degradation rates of −0.42%/year, −0.60%/year, and −0.71%/year, respectively.

A secondary point is plotted for this study in Figure 8 to represent the same selection criteria used in this work. Removing thin-film technologies, systems with field exposure <3 years, and systems in Dfa climate zones instead results in 13 PV systems with a median degradation rate of −0.19%/year.

In this work, we examined PV system degradation across continental and polar climate zones of Dfb, Dfc, and ET. We limited our literature review of cold climate degradation rates to only sites with ≥3 years of data and mc-Si or c-Si technologies to improve data quality and comparability. The median degradation rate was found to be −0.33%/year (−0.45%/year on average). This represents the most thorough report of cold climate degradation analysis to date, which includes tundra and subarctic climates.

5.3 | Data Limitations

A thorough understanding of long-term PV performance in cold climates is limited by the slower uptake of the PV industry at

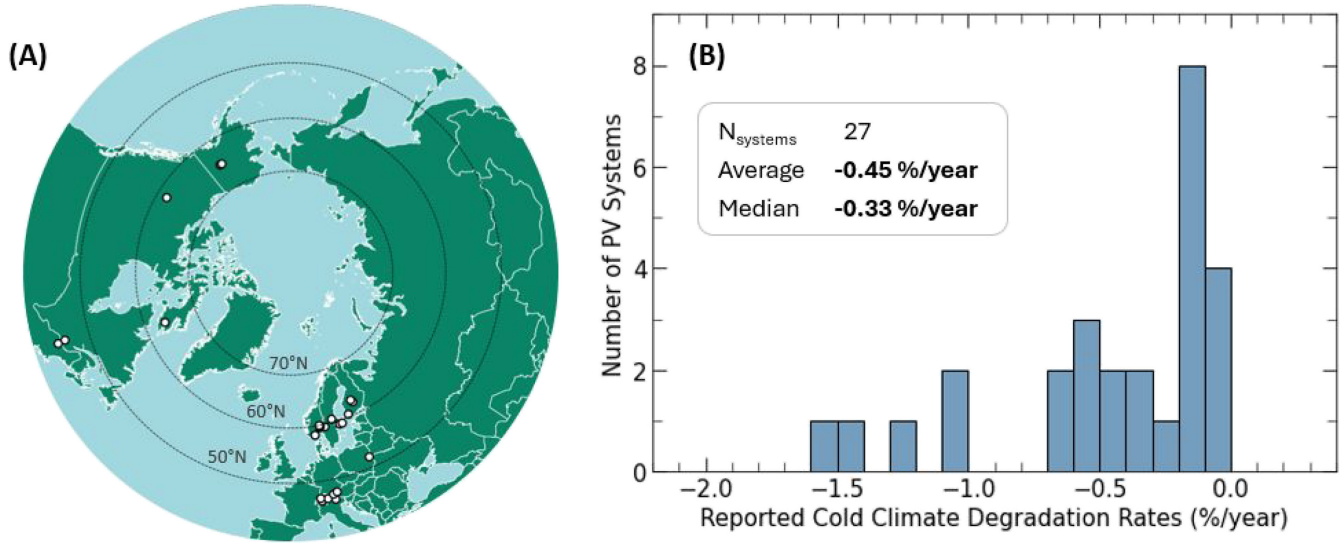

FIGURE 7 | (A) The location of reported degradation rates for all 27 mc-Si and c-Si PV systems with ≥3 years of field exposure in Dfb, Dfc, or ET climates. (B) The distribution of reported degradation rates in cold climates in this work covering Dfb, Dfc, and ET Köppen–Geiger climates. The sample size, average, and median are inset.

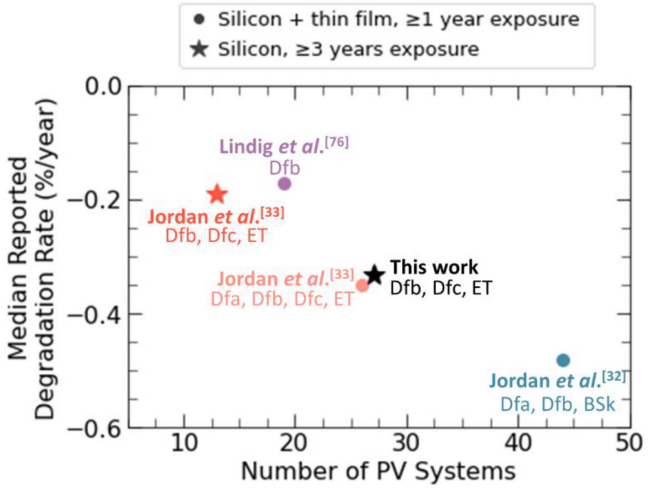

FIGURE 8 | Reported median degradation rates for cold climate locations in the literature. The Köppen–Geiger climate zones associated with each study are listed next to each reference point. Dfa and BSk represent warmer climate zones in the continental United States. Circles denote analysis that includes thin film technologies and PV systems with field exposure <3 years, whereas stars denote analysis of only silicon PV systems with ≥3 years of field exposure.

high latitudes and altitudes, compounded by a lack of collocated instrumentation near existing PV sites, sparse ground irradiance stations, and lower satellite data quality at high latitudes [76–78]. In the presented compendium, the degradation rates of 27 unique silicon PV systems in Dfb, Dfc, and ET climate zones are analyzed.

There are notable data gaps in the compendium relating to PV system configuration and location. PV systems with reported degradation rates in cold climates are typically small rooftop deployments with <10 years of field exposure. Furthermore, no reports on PV site degradation were found for Dfb, Dfc, or ET climates in Russia, Greenland, and several other countries, which may be due to limited PV deployments in these regions to date [79, 80].

Additionally, we observed a trend towards higher degradation rates for PV systems deployed in recent decades compared to systems deployed in the 1980s and 1990s. More data are required to corroborate this finding.

A few studies were found for PV systems in Eastern Europe and the United States that did not specify latitude and longitude coordinates, resulting in their exclusion from this analysis. However, these systems may be located in Dfb, Dfc, or ET Köppen–Geiger climate zones. Larrivee [81] reported the degradation rates of several PV systems in Germany. Belik et al. [82] reported degradation rates between −0.7% and −1.3%/year for unnamed c-Si PV plants in the Czech Republic and Ukraine. Murgescu et al. [83] reported the PLR of several PV plants in Romania without geographical coordinates. Finally, Raupp et al. [84] reported an average degradation rate of −0.7%/year for two rooftop systems in New York State, which may be located in a continental or temperate climate zone.

Nonetheless, the results presented in this review represent the most thorough compilation of degradation studies in Dfb, Dfc, and ET climates to date. Lessons learned from PV systems deployed in subarctic and tundra climates can inform the performance of PV systems in warmer climates, which are experiencing more frequent extreme weather events including heavy snowfall, ice storms, and high wind events [85].

6 | Conclusion

In this work, we presented a compendium of silicon PV system degradation rates in cold continental and polar Köppen–Geiger climate zones (Dfb, Dfc and ET) with ≥3 years of field exposure. The 27 PV sites presented have a median

degradation rate of −0.33%/year and an average degradation rate of −0.45%/year. Snow load, high winds, and freeze–thaw cycles with temperatures as low as −40°C can cause cell and frame strain and embrittlement in these climates. However, the benefits of lower PV system operating temperatures and reduced UV-light exposure are suspected to outweigh these mechanical stresses, leading to the overall lower observed degradation rates. PV systems deployed in subarctic and tundra climates can be expected to provide lasting power for high latitude and alpine communities.

A diverse range of methodologies for calculating degradation rates is present in the compendium, highlighting the variability of degradation analyses, and underscoring the need for standardized calculation methods to improve comparability and accuracy across future studies. Year-on-year approaches are recommended in particular for high-latitude locations that experience strong seasonality and remote locations that may be more prone to data outages.

New PV systems and test sites deployed in cold climates should collect and store data over the long term to facilitate reliability studies and regular degradation monitoring. This is particularly important in remote locations, where access to I-V flash testing equipment may be limited. However, long-term data collection in cold climates for year-on-year degradation analyses can be challenging in cold climates due to small regional PV workforces, outdoor operation and maintenance challenges in winter months, and higher data-outage potential. In the case where I-V tracing equipment is available, flash-testing modules before and after field exposure are recommended to supplement year-on-year methodologies or when continuous data collection is not possible.

Further studies on new bifacial technologies, such as SHJ and TOPCon modules, are required across different climate zones to determine their degradation rates and mechanisms under varied outdoor stressors. A trend towards higher degradation rates for PV systems deployed in recent decades is observed in the compendium, which may be due to larger and thinner module architectures in recent years. Continued development of reliability standards and testing is critical to maintaining module durability under cold climate stressors of snow load, wind load, and freeze–thaw cycles.

Finally, included in this review is the examination of three new subarctic ground-mounted PV sites > 60° N in Alaska and Canada using RdTools, representing the three highest latitude PV sites in the compendium and the first PV systems analyzed in Alaska for degradation. We show that the specific yield of these subarctic PV sites varied between 911 and 1329 kWh/kWp, depending largely on the system configuration and cell technology. Site PV power data availability was > 90% in all cases, whereas meteorological data experienced more outages, with availabilities of 65%, 84%, and 95%. For the 16-year-old double-axis tracking PV system located in Fairbanks, Alaska (65° N), the arrays demonstrated tracking availabilities of 48%–86%. The tracking of one of three arrays failed after 12 years of operation. Overall, the newly analyzed subarctic North American PV sites showcase a wide range of degradation rates from −0.4%/year to −1.5%/year due to their widely varying system configurations, module technologies, and deployment age.

Author Contributions

Erin M. Tonita: conceptualization, software, investigation, formal analysis, investigation, data curation, writing – original draft, writing – review and editing, visualization. **Dirk C. Jordan:** conceptualization, methodology, software, formal analysis, investigation, data curation, writing – review and editing, supervision. **Silvana Ovaitt:** conceptualization, writing – review and editing, supervision. **Henry Toal:** conceptualization, resources, data curation. **Karin Hinzer:** writing – review and editing, supervision, funding acquisition. **Christopher Pike:** conceptualization, resources, data curation, writing – review and editing, supervision. **Chris Deline:** writing – review and editing, supervision, funding acquisition.

Acknowledgments

The authors would like to extend their thanks to Qwerty Mackey and Robbin Garber-Slaght from the NREL's Alaska Campus for assistance with data curation for the double-axis tracking site in Fairbanks, Alaska. Thank you to the Northwest Territories Power Corporation and Christopher Baldus-Jeursen from CanmetENERGY for providing data for the PV site in Fort Simpson, Northwest Territories. Thank you to Kirsten Perry and Robert White from NREL for porting data and assisting with data cleaning routines. This work was authored in part by the University of Ottawa with the support of the Canadian Foundation for Innovation, Ontario Research Fund, and the Natural Sciences and Engineering Research Council of Canada (NSERC CREATE 497981, NSERC STPGP 521894, and NSERC CGS-D). The University of Ottawa is located on the unceded territory of the Anishinaabe Algonquin Nation. This work was authored in part by the Alaska Center for Energy and Power, University of Alaska Fairbanks, with funding additionally provided by the Department of Navy Award N00014-19-1-2235 issued by the Office of Naval Research. This work was also authored in part by the National Renewable Energy Laboratory (NREL), operated by Alliance for Sustainable Energy LLC, for the US. Department of Energy (DOE) under Contract No. DE-AC36-08GO28308. Partial funding is provided by the US Department of Energy (DOE)'s Office of Energy Efficiency and Renewable Energy (EERE) from the Solar Energy Technologies Office (SETO), under CPS Agreement 385258, and as part of the Durable Module Materials Consortium 2 (DuraMAT 2) funded by the US DOE, Office of EERE, SETO, Agreement Number 38259. The views expressed in the article do not necessarily represent the views of the DOE or the US Government. The US Government retains and the publisher, by accepting the article for publication, acknowledges that the US Government retains a nonexclusive, paid-up, irrevocable, worldwide license to publish or reproduce the published form of this work, or allow others to do so, for US Government purposes. The funders had no role in study design, data collection and analysis, decision to publish, or preparation of the manuscript.

Data Availability Statement

The data supporting the findings of this study are available publicly online and by request. Power data for Fort Simpson can be found publicly online by the Northwest Territories Power Corporation portal [40], whereas associated meteorological station data can be requested from CanmetENERGY. All data for the double-axis tracking site in Fairbanks maintained by NREL-Alaska (formerly the Cold Climate Housing Research Center) are publicly available [42]. Data are available upon request for the east–west vertical and south-tilted PV site in Fairbanks by reaching out to the Alaska Center for Energy and Power at the University of Alaska Fairbanks. RdTools is available as an open-source Python package for the calculation of year-on-year degradation rates and associated statistics [39].

References

1. U. Jahn and W. Nasse, "Analysis of Long-Term Performance and Reliability of Photovoltaic Systems," IEA Task 2 Draft Report (2003).

2. J. Hedström and L. Palmblad, "Performance of Old PV Modules: Measurement of 25 Year Old Crystalline Silicon Modules," Technical Report ELFORSK-01-71 (2006).

3. M. Lindh, "Country Report: Sweden," in 2024 High Latitude Photovoltaics Workshop, Piteå, Sweden (2024), https://www.sandia.gov/app/uploads/sites/243/dlm_uploads/2024/03/3.1-LindhMattias_Sweden_20240314.pdf.

4. E. S. Marstein, "Country Report: Norway," in 2024 High Latitude Photovoltaics Workshop, Piteå, Sweden (2024), 1–17, https://www.sandia.gov/app/uploads/sites/243/dlm_uploads/2024/03/3.2-Marstein-Norway-20240314-1.pdf.

5. S. Ranta, "PV Progress in Finland," in 2024 High Latitude Photovoltaics Workshop, Piteå, Sweden (2024), 1–15, https://www.sandia.gov/app/uploads/sites/243/dlm_uploads/2024/03/3.3-RantaSamuli-Finland-20240314.pdf.

6. E. Larsen, "Country Report: Denmark & Greenland," in 2024 High Latitude Photovoltaics Workshop, Piteå, Sweden (2024), 1–19, https://www.sandia.gov/app/uploads/sites/243/dlm_uploads/2024/03/3.4-LarsenEsben-Denmark-Greenland-20240314.pdf.

7. C. Pike, "High Latitude Solar Workshop Country Report: United States," in 2024 High Latitude Photovoltaics Workshop, Piteå, Sweden (2024), 1–11, https://www.sandia.gov/app/uploads/sites/243/dlm_uploads/2024/03/3.5-PikeChris-UnitedStates-20240314.pdf.

8. E. M. Tonita, "Status of PV in Canada," in 2024 High Latitude Photovoltaics Workshop, Piteå, Sweden (2024), 1–18, https://www.sandia.gov/app/uploads/sites/243/dlm_uploads/2024/03/3.6-TonitaErin_Canada_20240314.pdf.

9. M. Dhimish, "Performance Ratio and Degradation Rate Analysis of 10-Year Field Exposed Residential Photovoltaic Installations in the UK and Ireland," *Clean Technologies* 2 (2020): 170–183, https://doi.org/10.3390/cleantechnol2020012.

10. H. Haeberlin, "Grid Connected PV Plant Jungfraujoch (3454m) in the Swiss Alps: 10 Years of Trouble-Free Operation With Record Energy Yields," in *19th European Photovoltaic Solar Energy Conference* (2004).

11. H. Gholami, H. N. Røstvik, N. M. Kumar, and S. S. Chopra, "Lifecycle Cost Analysis (LCCA) of Tailor-Made Building Integrated Photovoltaics (BIPV) Façade: Solsmaragden Case Study in Norway," *Solar Energy* 211 (2020): 488–502, https://doi.org/10.1016/j.solener.2020.09.087.

12. A. Boute, "Off-Grid Renewable Energy in Remote Arctic Areas: An Analysis of the Russian Far East," *Review* 59 (2016): 1029–1037, https://doi.org/10.1016/j.rser.2016.01.034.

13. E. Usher, G. Jean, and G. Howell, "The Use of Photovoltaics in a Northern Climate," *Solar Energy Materials and Solar Cells* 34 (1994): 73–81, https://doi.org/10.1016/0927-0248(94)90026-4.

14. S. Rönnberg, M. Bollen, and A. Larsson, "Grid Impact From PV-Installations in Northern Scandinavia," in *2nd International Conference and Exhibition on Electricity Distribution (CIRED 2013)* (2013), 1–4, https://doi.org/10.1049/cp.2013.1046.

15. I. Das and C. A. Canizares, "Renewable Energy Integration in Diesel-Based Microgrids at the Canadian Arctic," *Proceedings of the IEEE* 107, no. 9 (2019): 1838–1856, https://doi.org/10.1109/JPROC.2019.2932743.

16. A. Wills, C. Banister, M. Pellissier, and J. Berquist, "A Multi-Year Analysis of Canadian Arctic Historical Weather Data in Support of Solar and Wind Renewable Energy Deployment," *E3S Web of Conferences* 246 (2021): 03006, https://doi.org/10.1051/e3sconf/202124603006.

17. D. Dumas and L. Gosselin, "Optimizing Photovoltaic Systems to Decarbonize Residential Arctic Buildings Considering Real Consumption Data and Temporal Mismatch," *Solar Energy* 275 (2024): 112560, https://doi.org/10.1016/j.solener.2024.112560.

18. S. V. Obydenkova and J. M. Pearce, "Technical Viability of Mobile Solar Photovoltaic Systems for Indigenous Nomadic Communities in Northern Latitudes," *Renewable Energy* 89 (2016): 253–267, https://doi.org/10.1016/j.renene.2015.12.036.

19. P. E. Campana, B. Stridh, T. Hörndahl, et al., "Experimental Results, Integrated Model Validation, and Economic Aspects of Agrivoltaics Systems at Northern Latitudes," *Journal of Cleaner Production* 437 (2024): 140235, https://doi.org/10.1016/j.jclepro.2023.140235.

20. L. Karttunen, S. Jouttijärvi, A. Poskela, et al., "Comparing Methods for Long-Term Performance Assessment of Bifacial Photovoltaic Modules in Nordic Conditions," *Renewable Energy* 219 (2023): 119473, https://doi.org/10.1016/j.renene.2023.119473.

21. E. Andenæs, B. P. Jelle, K. Ramlo, T. Kolås, J. Selj, and S. E. Foss, "The Influence of Snow and Ice Coverage on the Energy Generation From Photovoltaic Solar Cells," *Solar Energy* 159 (2018): 318–328, https://doi.org/10.1016/j.solener.2017.10.078.

22. D. Riley, L. Burnham, W. Snyder, B. King, and P. Dice, "Measurement of Snow Loading on a Tilted PV Module in Northern Michigan," in *IEEE 49th Photovoltaic Specialists Conference (PVSC)* (2022), 1343–1345, https://doi.org/10.1109/PVSC48317.2022.9938704.

23. J. D. Brearly, "Designing PV Systems for Environmental Extremes," *Solarpro Magazine* 8, no. 5 (2015): 1–8.

24. E. J. Schneller, H. Seigneur, J. Lincoln, and A. M. Gabor. "The Impact of Cold Temperature Exposure in Mechanical Durability Testing of PV Modules," in *IEEE 46th Photovoltaic Specialists Conference (PVSC)* (2019), 1521–1524, https://doi.org/10.1109/PVSC40753.2019.8980533.

25. U. Blieske and G. Stollwerck, "Chapter Four—Glass and Other Encapsulation Materials," *Semiconductors and Semimetals* 89 (2013): 199–258, https://doi.org/10.1016/B978-0-12-381343-5.00004-5.

26. M. D. Kempe, G. J. Jorgensen, K. M. Terwilliger, T. J. McMahon, C. E. Kennedy, and T. T. Borek, "Acetic Acid Production and Glass Transition Concerns With Ethylene-Vinyl Acetate Used in Photovoltaic Devices," *Solar Energy Materials and Solar Cells* 91, no. 4 (2007): 315–329, https://doi.org/10.1016/j.solmat.2006.10.009.

27. W. Hermann and N. Bogdanski, "Outdoor Weathering of PV Modules—Effects of Various Climates and Comparison With Accelerated Laboratory Testing," in *IEEE 37th Photovoltaic Specialists Conference (PVSC)* (2011), 2305–2311, https://doi.org/10.1109/PVSC.2011.6186415.

28. J. Lopez-Garcia, D. Pavanello, and T. Sample, "Analysis of Temperature Coefficients of Bifacial Crystalline Silicon PV Modules," *IEEE Journal of Photovoltaics* 8, no. 4 (2018): 960–968, https://doi.org/10.1109/JPHOTOV.2018.2834625.

29. M. Aghaei, A. Fairbrother, A. Gok, et al., "Review of Degradation and Failure Phenomena in Photovoltaic Modules," *Renewable and Sustainable Energy Reviews* 159 (2022): 112160, https://doi.org/10.1016/j.rser.2022.112160.

30. A. Sinha, H. Gopalakrishna, A. B. Subramaniyan, et al., "Prediction of Climate-Specific Degradation Rate for Photovoltaic Encapsulant Discoloration," *IEEE Journal of Photovoltaics* 10, no. 4 (2020): 1093, https://doi.org/10.1109/JPHOTOV.2020.2989182.

31. A. Omazic, G. Oreski, M. Halwachs, et al., "Relation Between Degradation of Polymeric Components in Crystalline Silicon PV Module and Climatic Conditions: A Literature Review," *Solar Energy Materials and Solar Cells* 192 (2019): 123–133, https://doi.org/10.1016/j.solmat.2018.12.027.

32. D. C. Jordan, K. Anderson, K. Perry, et al., "PV Fleets Degradation Insights," *Progress in Photovoltaics: Research and Applications* 30, no. 10 (2022): 1166–1175, https://doi.org/10.1002/pip.3566.

33. D. C. Jordan, S. R. Kurtz, K. VanSant, and J. Newmiller, "Compendium of Photovoltaic Degradation Rates," *Progress in Photovoltaics: Research and Applications* 24, no. 7 (2016): 978–989, https://doi.org/10.1002/pip.2744.

34. P. Ingenhoven, G. Belluardo, G. Makrides, et al., "Analysis of Photovoltaic Performance Loss Rates of Six Module Types in Five Geographical Locations," *IEEE Journal of Photovoltaics* 9, no. 4 (2019): 1091–1096, https://doi.org/10.1109/JPHOTOV.2019.2913342.

35. K. Kunaifi, A. Reinders, S. Lindig, M. Jaeger, and D. Moser, "Operational Performance and Degradation of PV Systems Consisting of Six Technologies in Three Climates," *Applied Sciences* 10, no. 16 (2020): 5412, https://doi.org/10.3390/app10165412.

36. T. Karin, C. B. Jones, and A. Jain, "Photovoltaic Degradation Climate Zones," in *IEEE 49th Photovoltaic Specialists Conference (PVSC)* (2019), 687–694, https://doi.org/10.1109/PVSC40753.2019.8980831.

37. R. Geiger and R. Ü. N. von Geiger, *Köppen-Geiger/ Klima der Erde. (Wandkarte 1:16 Mill.) – Klett-Perthes* (Gotha, 1961).

38. J. Ascencio-Vásquez, I. Kaaya, K. Brecl, K.-A. Weiss, and M. Topič, "Global Climate Data Processing and Mapping of Degradation Mechanisms and Degradation Rates of PV Modules," *Energies* 12 (2019): 4749, https://doi.org/10.3390/en12244749.

39. D. C. Jordan, C. Deline, S. R. Kurtz, G. M. Kimball, and M. Anderson, "Robust PV Degradation Methodology and Application," *IEEE Journal of Photovoltaics* 8, no. 2 (2018): 525–531, https://doi.org/10.1109/JPHOTOV.2017.2779779.

40. Northwest Territories Power Corporation, "Fort Simpson Solar Energy Project," website accessed June 28, 2024, (2024), https://www.ntpc.com/energy-alternatives/current-alternative-energy-projects/fort-simpson-solar-energy-project.

41. C. Pike, E. Whitney, M. Wilber, and J. S. Stein, "Field Performance of South-Facing and East-West Facing Bifacial Modules in the Arctic," *Energies* 14, no. 4 (2021): 1210, https://doi.org/10.3390/en14041210.

42. Cold Climate Housing Research Center, "RTF Solar PV," website accessed June 28, 2024, (2024), http://cchrc.rcs.alaska.edu.

43. R. Colgan, N. Wiltse, M. Lilly, B. LaRue, and G. Egan, "Performance of Photovoltaic Arrays—Cold Climate Housing Research Center (CCHRC)," (2010), CCHRC Snapshot RS 2010-10, https://cchrc.org/media/Solar_Photovoltaics.pdf.

44. M. Deceglie, A. Nag, A. Shinn, et al., "RdTools, Version 2.1.7, Computer Software," https://github.com/NREL/rdtools.

45. M. G. Deceglie, K. Anderson, D. Fregosi, et al., "Perspective: Performance Loss Rate in Photovoltaic Systems," *Solar RRL* 7, no. 15 (2023): 2300196, https://doi.org/10.1002/solr.202300196.

46. A. P. Dobos, "PVWatts Version 5 Manual," NREL/TP-6A20–62641, National Renewable Energy Lab, (2014), https://doi.org/10.2172/1158421.

47. K. Anderson, C. Hansen, W. Holmgreen, A. Jensen, M. Mikofski, and A. Driesse, "pvlib Python; 2023 Project Update," *Journal of Open Source Software* 8, no. 92 (2023): 5994, https://doi.org/10.21105/joss.05994.

48. M. J. Reno and C. W. Hansen, "Identification of Periods of Clear Sky Irradiance in Time Series of GHI Measurements," *Renewable Energy* 90 (2016): 520–531, https://doi.org/10.1016/j.renene.2015.12.031.

49. D. C. Jordan and C. Hansen, "Clear-Sky Detection for PV Degradation Analysis Using Multiple Regression," *Renewable Energy* 209 (2023): 393–400, https://doi.org/10.1016/j.renene.2023.04.035.

50. A. Phinikarides, N. Kindyni, G. Makrides, and G. E. Georghiou, "Review of Photovoltaic Degradation Rate Methodologies," *Renewable and Sustainable Energy Reviews* 40 (2014): 143–152, https://doi.org/10.1016/j.rser.2014.07.155.

51. E. Tonita, A. Russell, C. Valdivia, and K. Hinzer, "Optimal Ground Coverage Ratios for Tracked, Fixed-Tilt, and Vertical Photovoltaic Systems for Latitudes up to 75° N," *Solar Energy* 258 (2023): 8–15, https://doi.org/10.1016/j.solener.2023.04.038.

52. L. Burnham, D. Riley, B. Walker, and J. M. Pearce, "Performance of Bifacial Photovoltaic Modules on a Dual-Axis Tracker in a High-Latitude, High-Albedo Environment," in *IEEE 46th Photovoltaic Specialists Conference (PVSC)* (2019), 1320–1327, https://doi.org/10.1109/PVSC40753.2019.8980964.

53. D. C. Jordan, B. Marion, C. Deline, T. Barnes, and M. Bolinger, "PV Field Reliability Status—Analysis of 100 000 Solar Systems," *Progress in Photovoltaics: Research and Applications* 28 (2020): 739–754.

54. D. Jordan, D. B. Sulas-Kern, S. Johnston, et al., "High Efficiency Module Degradation—From Atoms to Systems," in *37th European Photovoltaic Solar Energy Conference* (2020), 828–833.

55. O. Arriaga Arruti, A. Virtuani, and C. Ballif, "Long-Term Performance and Reliability of Silicon Heterojunction Solar Modules," *Progress in Photovoltaics: Research and Applications* 31, no. 7 (2023): 664–677, https://doi.org/10.1002/pip.3688.

56. C. Deline, D. Jordan, B. Sekulic, J. Parker, B. McDanold, and A. Anderberg, "PV Lifetime Project—2024 NREL Annual Report," National Renewable Energy Laboratory, Golden, CO, NREL/TP-5K00-90651 (2024), https://www.nrel.gov/docs/fy24osti/90651.pdf.

57. R. H. French, L. S. Bruckman, D. Moser, et al., "Assessment of Performance Loss Rate of PV Power Systems," (2021), IEA PVPS Task 13, Report IEA-PVPS T13-22:2021, https://iea-pvps.org/key-topics/assessment-of-performance-loss-rate-of-pv-power-systems/.

58. C. Baldus-Jeursen, A. Côté, T. Deer, and Y. Poissant, "Analysis of Photovoltaic Module Performance and Life Cycle Degradation for 23 Year-Old Array in Quebec, Canada," *Renewable Energy* 174 (2021): 547–556, https://doi.org/10.1016/j.renene.2021.04.013.

59. H. Haeberlin and P. Schaerf, "Newtech—3 Different Thin Film PV Plants of 1kWp Under Direct Long-Term Comparison (2002–2009)," in *25th European Photovoltaic Solar Energy Conference* (2010).

60. N. Bogdanski, W. Herrmann, F. Reil, M. Köhl, K. A. Weiss, and M. Heck, "Results of 3 Years' PV Module Weathering in Various Open-Air Climates," *Proceedings SPIE 7773, Reliability of Photovoltaic Cells, Modules, Components, and Systems III, 77730L* (2010), https://doi.org/10.1117/12.859807.

61. H. Wilk, A. Szeless, A. Beck, H. Meier, M. Heikkilä, and C. Nyman, "Eureka Project EU 333 Alpsolar: Field Testing and Optimization of Photovoltaic Solar Power Plant Equipment, Progress Report 1994," *12th European Photovoltaic Solar Energy Conference (EUPVSEC)*, Amsterdam (1994).

62. A. Zdyb and S. Gulkowski, "Performance Assessment of Four Different Photovoltaic Technologies in Poland," *Energies* 13 (2020): 196, https://doi.org/10.3390/en13010196.

63. D. Verma, M. Tayyib, T. O. Saetre, and O. Midtgård, "Outdoor Performance of 10 Year Old a-Si and Poly-Si Modules in Southern Norway Conditions," in *IEEE 38th Photovoltaic Specialists Conference* (2012), 2368–2371, https://doi.org/10.1109/PVSC.2012.6318074.

64. B. R. Paudyal and A. G. Imenes, "Performance Assessment of Field Deployed Multi-Crystalline PV Modules in Nordic Conditions," in *46th IEEE Photovoltaic Specialists Conference (PVSC)* (2019), 1377–1383, https://doi.org/10.1109/PVSC40753.2019.8980629.

65. L. Palmblad, C. Martinsson, J. Hedstrom, and Andersson, M., "Long-Term Performance of PV Modules—Results From Swedish Case Studies," in *22nd European Photovoltaic Solar Energy Conference (EUPVSEC)* (2007).

66. M. Rinio, U. Enarsson, and C. Hansen, "A Fast Software Check for PV Systems," in *8th World Conference on Photovoltaic Energy Conversion* (2022), 1085–1088, https://doi.org/10.4229/WCPEC-82022-4DO.2.4.

67. E. B. Sveen, M. B. Øgaard, J. H. Selj, and G. Otnes, "PV System Degradation Rates in the Nordics," in *37th European Photovoltaic Solar Energy Conference (EUPVSEC)* (2020), 1563–1566.

68. C. Seiffert, *PV Module Degradation Rates in Norway* (High Latitude PV Workshop, 2024).

69. E. Psimopoulos, J. Plautz, F. Fiedler, and A. Augusto, "Performance of PV System Operating for 30-Years in Scandinavia," in *51st IEEE Photovoltaic Specialists Conference (PVSC)* (2024), https://doi.org/10.1109/PVSC57443.2024.10748925.

70. D. M. Mutungi, "Degradation of Photovoltaics in Central Finland: A Comparative Study of Polycrystalline and Heterojunction With Intrinsic Thin Layer Technologies" (Masters Thesis, University of Jyväskylä, 2013).

71. Y. Poissant, D. Thevenard, and D. Turcotte, *Performance Monitoring of the Nunavut Arctic College PV System: Nine Years of Reliable Electricity Generation*, CanmetENERGY (2004).

72. D. C. Jordan, C. Deline, M. Deceglie, T. J. Silverman, and W. Luo, "PV Degradation—Mounting & Temperature," in *46th IEEE Photovoltaic Specialists Conference (PVSC)* (2019), 673–679, https://doi.org/10.1109/PVSC40753.2019.8980767.

73. N. Bansal, S. P. Jaiswal, and G. Singh, "Comparative Investigation of Performance Evaluation, Degradation Causes, Impact and Corrective Measures for Ground Mount and Rooftop Solar PV Plants—A Review," *Sustainable Energy Technologies and Assessments* 47 (2021): 101526, https://doi.org/10.1016/j.seta.2021.101526.

74. J. Zuboy, M. Springer, E. C. Palmiotti, J. Karas, B. L. Smith, and M. Woodhouse, "Getting Ahead of the Curve: Assessment of New Photovoltaic Module Reliability Risks Associated With Projected Technological Changes," *IEEE Journal of Photovoltaics* 14, no. 1 (2024): 4–22, https://doi.org/10.1109/JPHOTOV.2023.3334477.

75. S. Lindig, D. Moser, A. J. Curran, and R. H. French, "Performance Loss Rates of PV Systems of Task 13 Database," in *46th IEEE Photovoltaic Specialists Conference (PVSC)* (2019), 1363–1367, https://doi.org/10.1109/PVSC40753.2019.8980638.

76. N. Matsui, C. N. Long, J. Augustine, et al., "Evaluation of Arctic Broadband Surface Radiation Measurements," *Atmospheric Measurement Techniques* 5, no. 2 (2012): 429–438, https://doi.org/10.5194/amt-5-429-2012.

77. B. Babar, L. T. Luppino, T. Boström, and S. N. Anfinsen, "Random Forest Regression for Improved Mapping of Solar Irradiance at High Latitudes," *Solar Energy* 198 (2020): 81–92, https://doi.org/10.1016/j.solener.2020.01.034.

78. H. N. Riise, M. M. Nygård, B. Aarseth, A. Dobler, and E. Berge, "Benchmark of Modelled Solar Irradiance Data at High Latitude Locations," SSRN Preprint (2024), https://doi.org/10.2139/ssrn.4804004.

79. M. Ross and J. Royer, "PV-Hybrid Power Systems for Radio Links in Greenland," in *Photovoltaics in Cold Climates*, 1st ed. (Routledge, 1998), 126–127.

80. A. Pantaleo, M. R. Albert, H. T. Snyder, S. Doig, T. Oshima, and N. E. Nagelqvist, "Modeling a Sustainable Energy Transition in Northern Greenland: Qaanaaq Case Study," *Sustainable Energy Technologies and Assessments* 54 (2022): 102774, https://doi.org/10.1016/j.seta.2022.102774.

81. J. Larrivee, "An Analysis of Degradation Rates of PV Power Plants at the System Level" (Masters Thesis, Utrecht University, 2013).

82. M. Belik, J. Timr, and O. Rubanenko, "Prediction of the Degradation Process of Mono-Si Photovoltaic Panels in Ukrainian and Czech Conditions," in *23rd International Scientific Conference on Electric Power Engineering (EPE)* (2023), 1–6, https://doi.org/10.1109/EPE58302.2023.10149312.

83. I. Murgescu, L. A. El-Leathey, and R. A. Chihaia, "Guaranteed Versus Real Service Life of PV Panels in Romania," *Journal of Engineering Sciences and Innovation* 3, no. 4 (2018): 375–392, https://doi.org/10.56958/jesi.2018.3.4.375.

84. C. Raupp, C. Libby, S. Tatapudi, et al., "Degradation Rate Evaluation of Multiple PV Technologies in 59,000 Modules Representing 252,000 Modules in Four Climatic Regions of the United States," in *IEEE 43rd Photovoltaic Specialists Conference (PVSC)*, Portland OR, USA, (2016), 255–260, https://doi.org/10.1109/PVSC.2016.7749590.

85. M. Bošnjaković, M. Stojkov, M. Katinić, and I. Lacković, "Effects of Extreme Weather Conditions on PV Systems," *Sustainability* 15, no. 22 (2023): 16044, https://doi.org/10.3390/su152216044.

Supporting Information

Additional supporting information can be found online in the Supporting Information section.